CEAS Aeronautical Journal (2023) 14:353–368
https://doi.org/10.1007/s13272-023-00650-5

ORIGINAL PAPER

Estimating vertiport passenger throughput capacity for prominent eVTOL designs

Lukas Preis[1]

Received: 16 May 2022 / Revised: 25 January 2023 / Accepted: 27 February 2023 / Published online: 6 May 2023

Abstract

Urban Air Mobility has the potential to substantially reduce travel times in some cases of urban-related transportation. Travel time savings strongly depend on fast processing at vertiports, which presents a key challenge considering demand levels' vertiports would experience when becoming an established mode of transport. This article sheds light on the passenger throughput vertiport airfields can manage and how the operations are sensitive to changes. One main contribution of this article is the introduction of hourly passenger throughput per area as a performance indicator that allows to compare vertiports of different sizes. VoloCity is studied as a reference vehicle and the resulting space requirement of the carefully specified baseline scenario is 188 square-meters per passenger per hour. A total of 13 prominent eVTOL designs are included in the study from which the current design space between maximum vehicle dimension and number of seats is deducted. The study shows that vehicles with a small maximum dimension yield the highest passenger throughput capacity. CityAirbus performs best (46.3 m^2/PAX/h) with a diameter of 7.92 m and Archer Maker performs worst (221 m^2/PAX/h) with a diameter of 12.2 m. How the performance indicators can be used as rules-of-thumb in the first-order estimations of vertiport throughput capacity or space requirement is described by means of illustrative examples. The insights presented in this paper might be useful for researches, vehicle developers, and municipalities alike.

Keywords urban air mobility · vertiport · throughput · evtol · space demand

Abbreviations

eVTOL	Electric vertical take-off and landing vehicle
FATO	Final approach and take-off area
MIP	Mixed-integer programming
TLOF	Touch down and lift-off area
UAM	Urban air mobility
VSM	Vertiport sizing method

List of Symbols

A	Area of vertiport airfield
n	Number of seats in eVTOL
σ_{pax}	Standard deviation of hourly passenger throughput per area
σ_A	Standard deviation of area demand per hourly passenger throughput
TP_{veh}	Vehicle throughput per hour
TP_{pax}	Passenger throughput per hour
tp_{pax}	Hourly passenger throughput per area
tp_A	Area demand per hourly passenger throughput

1 Introduction

Urban Air Mobility (UAM) is an emerging transportation concept that has the potential to enrich the existing transport system through a new mode with the particular advantage of reducing travel times. The introduction of UAM faces several hurdles [1], among which infrastructure has been identified as a key issue by NASA [2], DLR [3], and MIT [4, 5]. Next to the aircraft-specific issues around Electric Vertical Take-Off and Landing Vehicles (eVTOL) [6–9], there are various hurdles to overcome, such as air traffic management [10–18], noise [19–22], or safety and certification [23–25]. Many of these issues are already being addressed as documented by various literature reviews and white papers [26–29], while the question of ground infrastructure only finds secondary attention. In particular, the locating and throughput capacity of vertiports has recently been identified as a significant research gap [30]. Reference [31] established that the comparatively small volume of research available

✉ Lukas Preis
Lukas.preis@tum.de

[1] Technical University of Munich, Munich, Germany

on vertiports is centrally focused on airspace operations and design; throughput capacity and ground operations have received less attention.

This paper wants to fill the research gap between the known importance of UAM ground infrastructure and the lack of insight into vertiport throughput capacity. For this purpose, an existing Vertiport Sizing Method (VSM) [32] (see Sect. 2) is applied first to a baseline scenario using *VoloCity* as reference vehicle and various sizes of vertiports (see Sect. 3) and second to a study contrasting prominent eVTOL designs (see Sect. 4). Performance indicators are defined to measure passenger throughput (see Sect. 3.2).

At the heart of all considerations is the idea of hourly throughput per area. Space in cities is a valuable commodity and therefore land use a relevant performance indicator. This approach has been used in the past for other modes of transport, showing that rail needs less space per passenger than cars [33]. Taking Germany as an example where 5% of the total land area is dedicated to transport [34], one can find the following space demand per daily passenger: 65 m^2 for cars, 32 m^2 for rail, and 620 m^2 for airplanes (the numbers were calculated by comparing statistics from the German Federal Statistical Office for land use [35] and passenger transport [36]). A direct comparison of these existing space demands with the estimated space demands for eVTOLs can be found in Appendix A.5.

2 Literature review and previous work

In a previous publication, a Mixed-Integer Programming (MIP) approach for sizing and designing vertiports has been presented [32]. The present work applies this MIP approach to analyze vertiport airfield passenger throughput capacities and expands the preliminary studies of [37]. Further publications that should find mention are Vascik's ground-breaking analysis of vertiport capacity envelopes, which served as inspiration for the MIP approach [38]. Another important work is by Zelinski, who looked at vertiport design in a holistic sense, considering among other things weather impact and vertiport topologies

Fig. 1 Definition of the vehicle throughput process

[39]. Reference [40] studied vertiport configurations for the Cologne-Bonn airport and determines a capacity of 9.6 aircraft movements per hour for the specific use case. Reference [41] developed a method to estimate the cost of various vertiport layouts and state an average of 420 m^2 per hourly vehicle throughput (for a direct comparison with the results of this article, see Appendix A.5). A patent for dynamic vertiport configurations was published by Ref. [42] and efforts to craft an ISO standard for vertiports is under way [43]. Further studies exploring different vertiport layouts and sizes were published by Deloitte [44], Lilium [45], and McKinsey [46].

Here, the VSM published by Preis [32] will be re-iterated briefly. The VSM uses MIP in a branch-and-bound fashion with a utility function of maximizing hourly vehicle or passenger throughput. Vehicle throughput is defined as the number of vehicles being able to complete the following process within 1 h: (1) approach of a vehicle from the airspace and landing on a pad, (2) taxiing to a gate, (3) turnaround at the gate including passenger boarding and de-boarding, (4) taxiing back to a pad, and (5) take-off and departure into the airspace (see Fig. 1). The passenger throughput, which will be the main unit of measurement in this paper, is formed by multiplying the vehicle throughput with the number of seats. Beneath this definition lies the assumption of a load factor of 1.0. Based on the size and shape of a given surface area, the optimal vertiport airfield layout is determined including the number of pads and gates, a suggestion for the topology, and the maximum possible hourly throughput. There are four topologies, which are compared for each scenario: single-pad, satellite, linear, and pier (see Fig. 2). Each topology follows a list of geometric rules, which are detailed by Hack Vazquez [47]. One geometric rule forces pads to be lined up

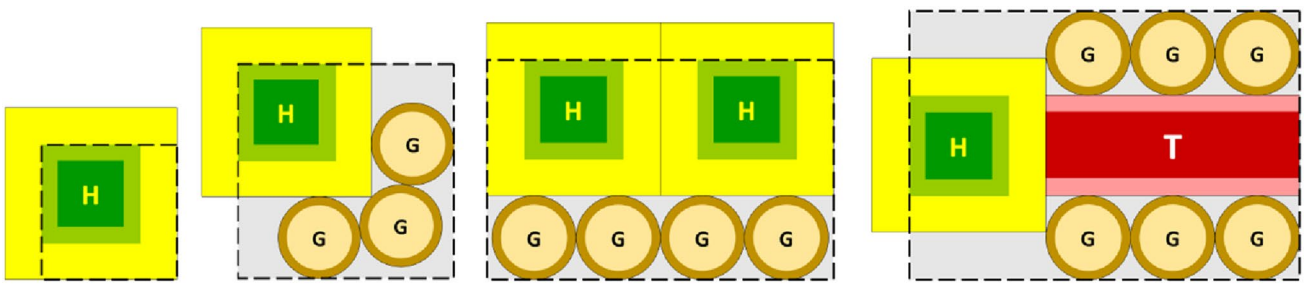

Fig. 2 Vertiport topologies considered in the vertiport sizing method: single-pad, satellite, linear, and pier

along the rim of the surface to ensure obstacle free approach and departure paths.

Assumptions for the pads are taken from the recently published *Engineering Brief No. 105, Vertiport Design* by FAA [48]. The report states that "in future guidance, parking and taxi-ways guidance will be included; if necessary in the interim, […] vertiport design should follow taxiway guidance in AC 150/5390-2". Therefore, the assumptions for the dimensions of gates and taxi-ways, including their safety zones, are derived from the "Heliport Design Guidelines" published by the *Advisory Circle 150/5390-2C* of the FAA [49]. Similar considerations are currently under way from EASA with a *Means of Compliance SC-VTOL* [50] while giving less details for airfield layouts and thereby yielding less utility for my article. A systematic discussion of historic and present vertiport design guidelines can be found in Ref. [31].

3 Baseline scenario and throughput performance

3.1 Definition baseline scenario

The operational parameters required by the VSM are shown in Table 1 and the values are chosen according to previous vertiport parameter specification [51] and aggregation [52]. The parameter values were determined through literature review and an expert interview series ($n = 17$) with participants from academia and industry. Approach & landing and take-off & departure of vehicles are each aggregated into one parameter and correspond to the time a pad is occupied with the respective operation (see Appendix A.1 for details on the value aggregation). As reference vehicle, the *VoloCity* from Volocopter was chosen (see Fig. 3) with two seats and a maximum dimension of 11.3 m [53]. The taxi-mode is "hovering close to the surface" with engines being shut-off after touch-down at the gate. For simultaneous operations of pads, the distance between their two Final Approach and Take-Off Area (FATO) must be at least 200 *ft* according to the heliport design guidelines by FAA [49]. All parameter values are listed in Table 1.

Fig. 3 *VoloCity* with two seats and 11.3 m maximum vehicle dimension (picture taken from 2021 Volocopter white paper [29])

Table 1 Input parameters required by vertiport sizing method including parameter value specification according to Preis et al. [50]; aggregated values are explained in Appendix A.1

Parameter	Value
Approach and landing time	99.2 s
Taxi speed	3.25 m/s
Taxi mode	Hover
Start/stop engines time	4.75 s
Passenger boarding time	92.7 s
Passenger de-boarding time	92.5 s
Take-off and departure time	72.2 s
Maximum dimension vehicle	11.3 m
Minimum distance FATO/FATO	200 ft (61 m)
Number of passengers	2
Vehicle turnaround time at gate	30 min

The baseline scenario has a turnaround time of 30 min, which might entail charging, battery swapping, or minor maintenance activities. It is assumed that vehicle-related turnaround and passenger boarding can happen simultaneously at the gate; the longer time of both determines to overall turnaround time. The total boarding time is the boarding and de-boarding time of one passenger multiplied by the number of seats. The load factor of each vehicle is assumed to be 1.0: during each turnaround, all passengers de-board the aircraft and new passengers board the aircraft until all seats are occupied. The length of the passenger-related turnaround has corresponding duration.

As illustration of the VSM process, Fig. 4 is included. Using the parameters outlined in Table 1 and giving an exemplary area of 6100 m^2 with a rectangular shape and an aspect ratio of 1:2, a passenger throughput of 32 per hour is possible. The optimal ratio of gates to pads and the spatial layout is computed for the four different topologies (single-pad, satellite, linear, and pier) as described in Sect. 2. Finally, the highest performing topology is selected, which is the linear topology in this case using nine gates per pad.

3.2 Definition of throughput performance indicator

Scenarios will be measured and compared based on the performance indicator of "hourly passenger throughput per area" tp_{pax} and its reciprocal "area demand per hourly passenger throughput" tp_A (see Eqs. 1 and 2, respectively). First, vehicle throughput TP_{veh} is defined according to the chain of processes shown in Fig. 1: "vehicle throughput of one per hour" means that the listed operations (arrival, taxi to gate, turnaround including boarding, taxi to pad, and departure) can take place once within 1 h on the given

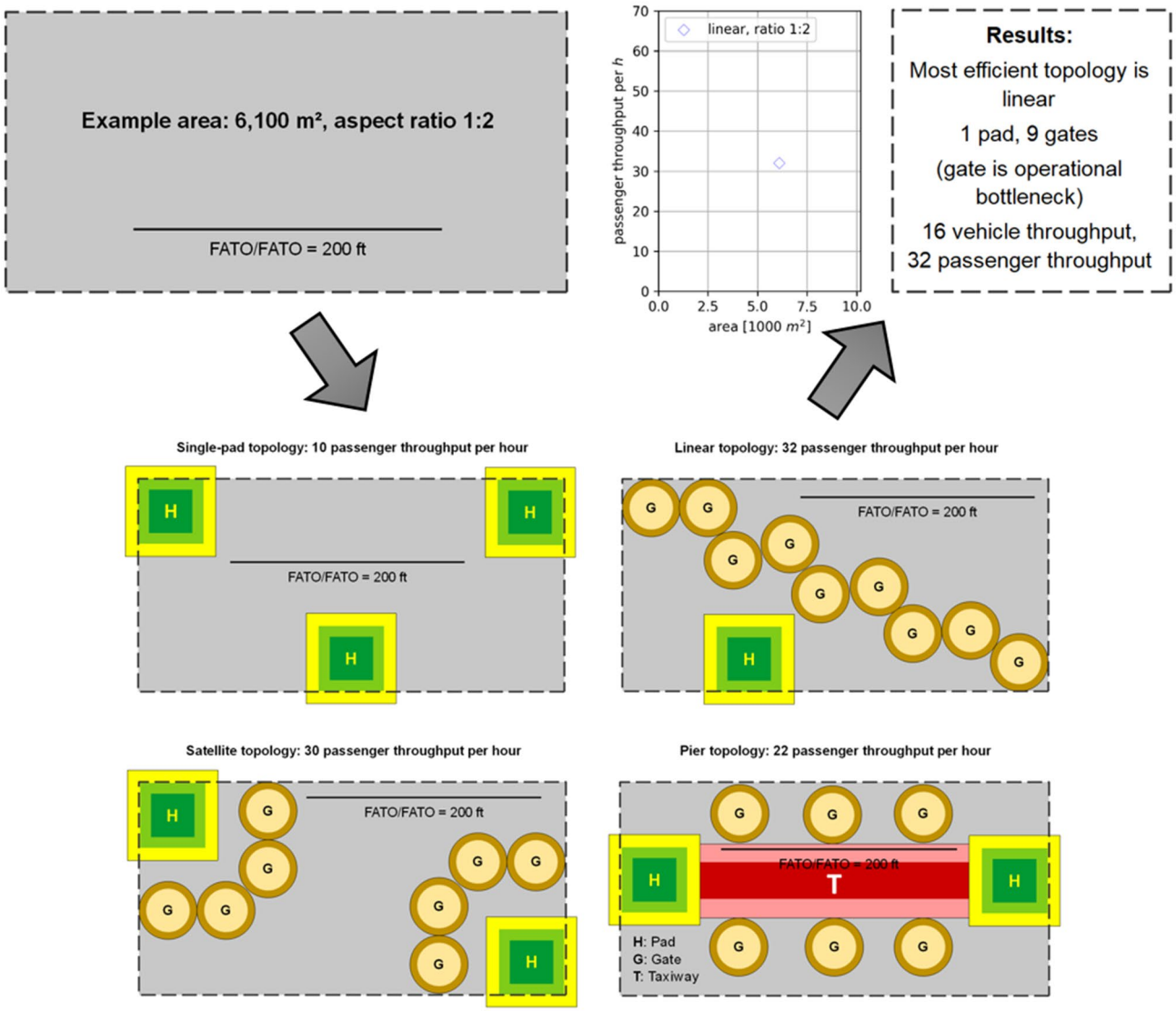

Fig. 4 Illustration of vertiport sizing process identifying the optimal vertiport airfield layout and estimating the passenger throughput capacity

vertiport airfield. The passenger throughput per hour TP_{pax} is TP_{veh} multiplied by the number of seats n in the vehicle. It should be explicitly mentioned that the number of seats (including the pilot seat) and not the number of passengers are counted to allow for comparison between piloted and autonomous eVTOL designs. In other words, the implicit assumption is autonomous eVTOLs as the number of seats and number of passengers are equated. Next, TP_{pax} is divided by the area of the vertiport airfield A. This yields the performance indicator "hourly passenger throughput per area" tp_{pax}, as shown in Eq. 1. This indicator allows for direct comparison between vehicles and different sizes of vertiports and will be used throughout this paper. To make the performance indicator more intuitive, the reciprocal of tp_{pax} is introduced alongside: "area demand per hourly passenger throughput" tp_A (see Eq. 2)

$$tp_{pax}\left[\frac{pax}{h * m^2}\right] = \frac{TP_{pax}\left[\frac{pax}{h}\right]}{A\left[m^2\right]}, with TP_{pax} = TP_{veh} * n \tag{1}$$

$$tp_A\left[\frac{m^2}{pax/h}\right] = \frac{A\left[m^2\right]}{TP_{pax}\left[\frac{pax}{h}\right]}. \tag{2}$$

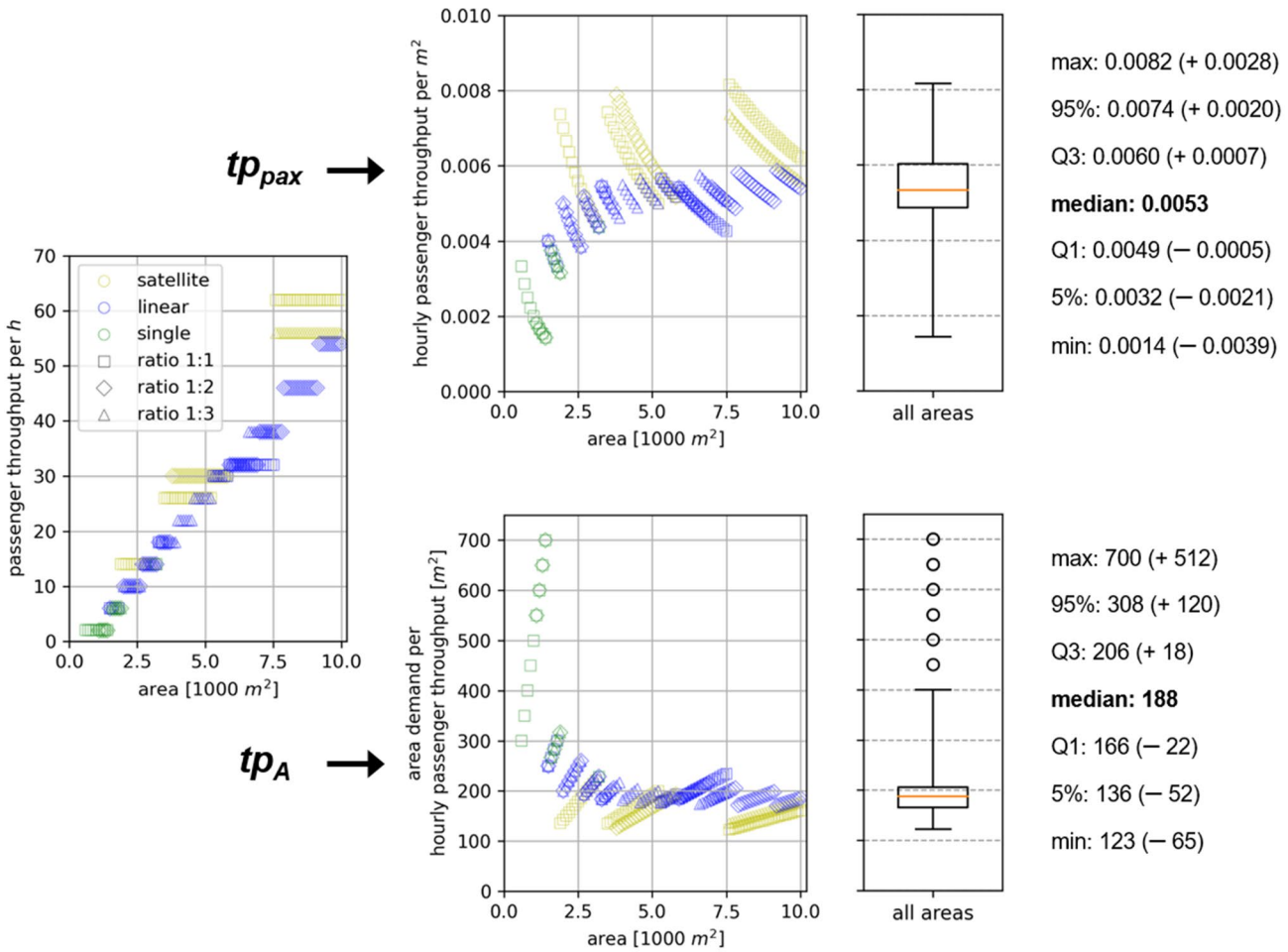

Fig. 5 Forming the throughput performance indicators and aggregating them into rules-of-thumb

How the performance indicators tp_{pax} and tp_A are formed is illustrated in Fig. 5. The passenger throughput per hour is shown on the left side displaying the area, throughput, aspect ratio of the area, and the best-performing topology for each scenario. Hourly passenger throughput per area tp_{pax} normalizes the throughput against the area and the area demand per hourly passenger throughput tp_A normalizes the area against the throughput. Finally, both indicators are condensed into a single boxplot as shown on the right. The interpretation and application of the performance indicators are discussed in Sect. 3.3 and Appendix, respectively.

3.3 Evaluation of baseline scenario

The baseline scenario as defined in Sect. 3.1 was simulated with the *VoloCity* as reference vehicle for areas from 100 to 10,000 m^2. The step size between areas is 100 m^2 and each area was considered in three variations as rectangles with aspect ratios 1:1, 1:2, and 1:3, yielding a total of 300 scenarios. Expressing the results in a rule-of-thumb, the median value of all scenarios is calculated for both throughput performance indicators. For the baseline scenario, the values are $tp_{pax} = 0.0053$ PAX/h/m^2 and $tp_A = 188$ m^2/PAX/h. The process of forming these rules-of-thumb is illustrated in Fig. 5 (the same process will be repeated for various prominent eVTOLs in Sect. 4.2 and is visualized for *eHang 216* and *Joby S4* in Appendix A.2). As the nature of vertiport airfield elements (pads, gates, etc.) is discrete (one cannot add half a pad), so will the results also be discrete. The discrete characteristic becomes apparent in the following plots where the norm is value—"jumps" instead of continuity.

Further, the gate-to-pad ratio will be discussed, as shown in Fig. 6, and how size and shape of an area influence both the optimal gate-to-pad ratio and the ideal topology. While single-pad topologies are best suited for small areas, there is a near-even split for medium and large areas between satellite and linear topologies. Pier topologies are at no point optimal within the scope of the study (in related studies, it

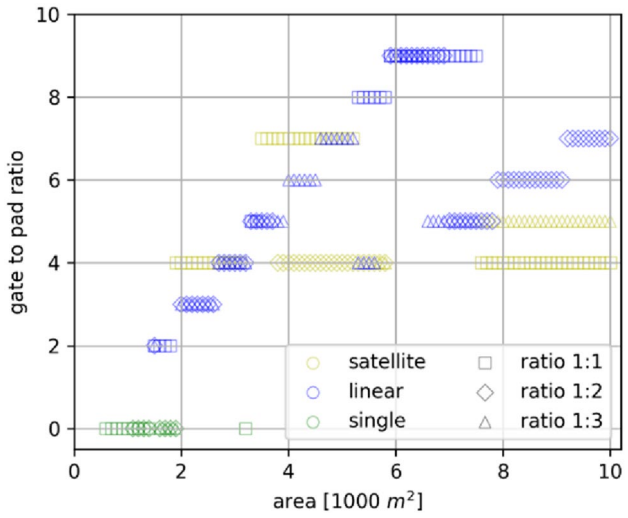

Fig. 6 Correlation between the size and shape of a given area, the optimal gate-to-pad ratio, and the best-performing topology

was observed that pier topologies grow in importance for short turnaround times and larger areas). Scenarios that favor satellite topologies seem to prefer a gate-to-pad ratio of 4 or 5. Scenarios that favor linear topologies can range from 2 to 9 gates per pad. There are two separate trends visible for the linear topology, which can be explained by a particular geometric rule: if the size and shape of an area allow for it, a linear topology can add a second row of pads and gates; the jump from one to two rows explains the two separate groups of linear topologies. Other than that, no clear trends are observable, which indicates the uniqueness of each scenario.

In a second step, the charging time of the baseline scenario of 30 min is varied to understand the impact of the turnaround time at the gate. The variations are no charging time (which means that only passenger boarding takes place at the gates) and 60 min charging time. The former can be interpreted as a touch-and-go "verti-stop" in a strongly space constrained inner city environment, and the latter as a "verti-hub" outside the city with extensive parking and maintenance facilities. Hourly passenger throughput per area is listed in Table 2 and area demand per hourly passenger throughput is listed in Table 3. How these numbers can be applied to the first-order estimations of either throughput capacity or area demand is exemplified in Appendix A.3.

Table 2 Passenger throughput performance of *VoloCity* according to "hourly passenger throughput per area"

Variance of performance [PAX/h/m^2]	No charging (boarding only)	30 min charging	60 min charging
Maximum	0.0240	0.00816	0.00395
95th percentile	0.0189	0.00737	0.00349
3rd quartile	0.0150	0.00603	0.00286
Median	0.0123	0.00533	0.00264
1st quartile	0.0101	0.00486	0.00236
5th percentile	0.00790	0.00325	0.00133
Minimum	0.00693	0.00143	0.00105

Table 3 Passenger throughput performance of *VoloCity* according to "area demand per hourly passenger throughput"

Variance of performance [m^2/PAX/h]	No charging (boarding only)	30 min charging	60 min charging
Maximum	144	700	950
95th percentile	127	308	750
3rd quartile	99.3	206	424
Median	81.1	187	379
1st quartile	66.7	166	350
5th percentile	52.8	136	287
Minimum	41.7	123	253

4 Study of prominent eVTOL designs

There are many ongoing eVTOL development projects of which the most mature and promising vehicles will be compared according to their operational performance in this section. The performance indicators tp_{pax} and tp_A will be used as explained in Sect. 3.2. A total of 13 vehicles were chosen, which are either prominent in the scientific literature or are close to receiving flight certification. For an extensive treatment of eVTOL development projects, please refer to Refs. [6–9].

4.1 Vehicle dimensions and seats

eVTOLs come in many different configurations: the three most prominent are multicopter, lift + cruise, and tilt-wing/prop configurations. Thirteen vehicles, including their dimensions and number of seats, are shown Table 4. Taking the seat per maximum dimension ratio as a measure of operational performance, the *CityAirbus* and the *Lilium Jet* perform best and *Archer Maker*, *Wisk Cora*, and the previously considered *VoloCity* perform worst. For reasons of comparability between autonomous and (human) piloted configurations, the pilot seat is counted among the total seats.

The design space derived from the collection of eVTOLs is shown in Fig. 7. The lower end is marked by a straight line going through the coordinate origin with a slope of 2 m per seat. The left end is marked by various vehicles with two

Table 4 Operations-related characteristics of prominent eVTOL designs

Name	Maximum dimension [m]	Total seats	Seats per maximum dimension [1/m]	Source
CityAirbus	7.92	4	0.51	[54]
VoloCity	11.3	2	0.18	[53]
Joby S4	10.7	4	0.37	[55]
Vahana (defunct)	6.25	2	0.32	[56]
Wisk Cora	11.0	2	0.18	[57]
eHang 216	5.63	2	0.36	[58]
UBER (concept)	15.2	5	0.33	[59]
ALIA-250	15.2	6	0.39	[60]
Lilium Jet	13.9	7	0.50	[61]
Archer Maker	12.2	2	0.16	[62]
Bell Nexus 4EX	12.2	5	0.41	[63]
Pipistrel 801	13.7	5	0.36	[64]
Autoflight V1500	12.8	4	0.31	[65]

seats; among the prominent designs, no single-seat vehicle was found. The upper end is marked by a straight line cutting through 13 m maximum dimension at two seats with an upward slope of 1 m per seat. The largest vehicles are under 16 m maximum dimension.

Next to the vehicle characteristics, the dimensions of the airfield elements (pads, gates, and taxi-ways) are driving the vertiport layout and throughput. The dimensions according to FAA heliport guidelines [49] are discussed in Appendix A.4.

4.2 Prominent vehicle study results

The study from Sect. 3.1 which is based on the *VoloCity* was executed analogous to the baseline scenario for all 13 vehicles listed in Table 4. It should be mentioned that none of the mentioned eVTOLs is certified for passenger transport, yet. How realistic the concepts are is not included in the study (except for the a prior focus on "prominent" eVTOL designs) and the certification process will weed out unfeasible vehicles. The design space presented in this paper and the results might therefore shift as time progresses. The results of the prominent eVTOL design study will be visualized and discussed in the following.

A linear approximation of the passenger throughput per hour for areas between 100 and 10,000 m^2 and all 13 eVTOLs can be seen in Fig. 8. The throughput performance indicators tp_{pax} and tp_A (see Sect. 3.2 for the definition of the performance indicators) are then visualized in Figs. 9 and 10 and contrasted in Table 5. Further, the standard deviations for both performance indicators, σ_{pax} and σ_A, are listed in the table to indicate the level of statistical reliability. It can be seen that *CityAirbus*, *eHang 216*, and *Vahana* perform best while also being the smallest vehicles. At this point, it needs to be emphasized that passenger throughput (not vehicle throughput) is used as performance indicator. With this in mind, it appears that the penalty of reduced throughput for a larger vehicle dimension outweighs the benefit of placing more seats in the same vehicle. Therefore, it can be inferred that small vehicles—independent of their small number of seats—create the highest throughput capacity. This effect can be traced back to the following: when operating small eVTOLs, the footprint of pads and gates is also small wherefore more pads and gates can be placed on the same area creating higher throughput capacity. The increase in operational complexity, which could be a limiting factor, is not accounted for in the present study. This insight is somewhat counter-intuitive, as aviation tends to employ larger aircraft with more seats where high throughput is demanded.

The presented performance indicators "hourly passenger throughput per area" and "area demand per hourly passenger throughput" allow for direct comparison of existing eVTOL designs—which, admittedly, could be a decisive issue. Therefore, two cautionary remarks about the interpretation of the results should be provided. First, the results depend strongly on two numbers: the vehicle dimension and number of seats. These numbers were, for the most part, taken directly from the manufacturer's websites and correspond to what the companies communicate with the public. Now, if eVTOL designs change, or the published numbers do not match the actual designs, the results would also change. Second, the throughput capacity on the vertiport is only one of many possible performance indicators to judge eVTOLs. Often used performance metrics are, for examples, speed, range, and payload. Yet, because space in inner city environments will be costly, the throughput capacity is an important metric to assess eVTOLs. A combined assessment of performance metrics will be published in a follow-up article as described in Sect. 6.

In Appendix, examples are given how tp_{pax} and tp_A can be applied as rules-of-thumb to do the first-order estimations for vertiport sizing. tp_{pax} can be used to estimate the possible hourly passenger throughput on a given area and tp_A can be used to determine the space requirement for a desired throughput capacity. Further, in Appendix A.5, the space requirements presented in Table 5 are compared to other modes of transport, such as rail, car, and commercial aviation.

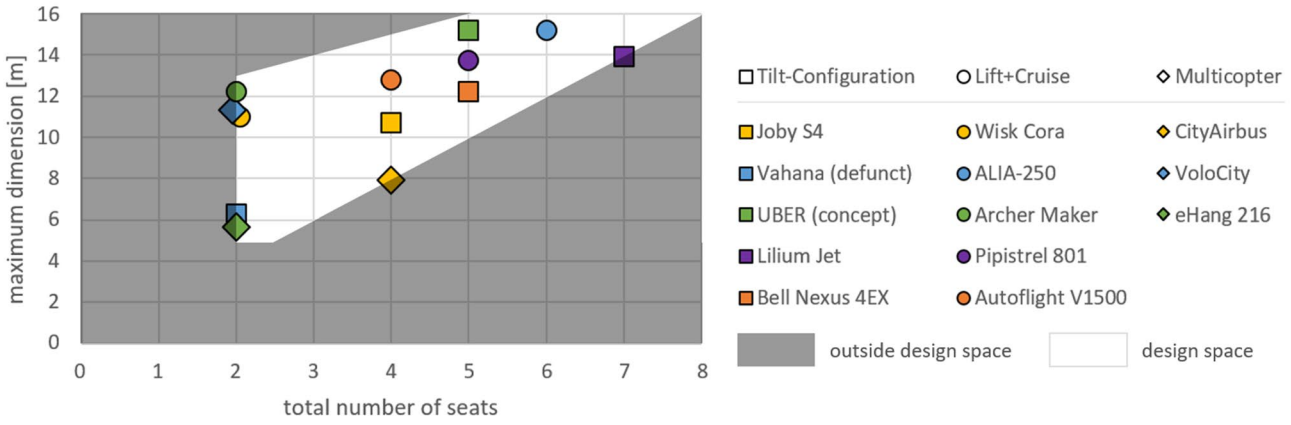

Fig. 7 Design space between maximum dimension of eVTOL and total number of seats

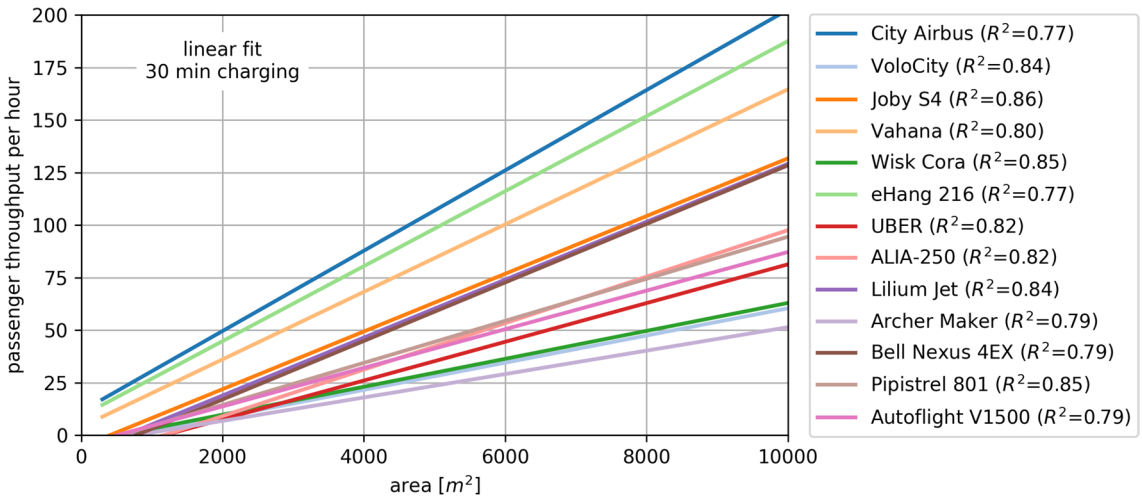

Fig. 8 Passenger throughput per hour depending on area of airfield for prominent eVTOLs

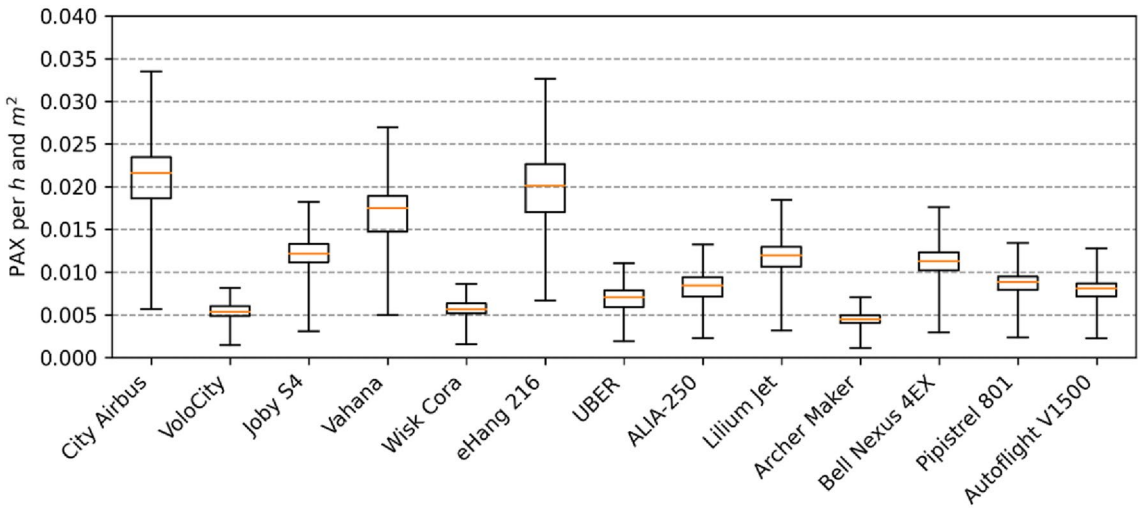

Fig. 9 Hourly passenger throughput per area and variance of values

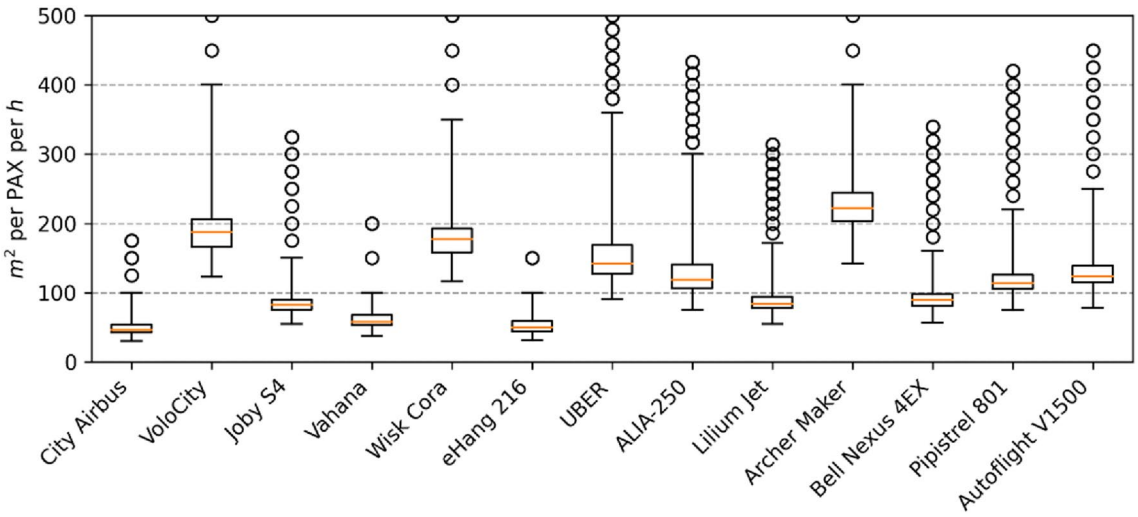

Fig. 10 Area demand per hourly passenger throughput and variance of values

Table 5 Operational eVTOL performance according to "hourly passenger throughput per area" and "area demand per hourly passenger throughput" (charging time 30 min)

Name	tp_{pax} [PAX/h/m^2]	σ_{pax} [PAX/h/m^2]	tp_A [m^2/PAX/h]	σ_A [m^2/PAX/h]
City Airbus	0.0216	0.0043	46.3	16.9
VoloCity	0.00533	0.0012	188	87.1
Joby S4	0.0121	0.0027	82.4	39.7
Vahana	0.0175	0.0032	57.3	16.8
Wisk Cora	0.00565	0.0013	177	78.4
eHang 216	0.0201	0.0040	49.7	12.7
UBER	0.00705	0.0020	141	85.1
ALIA-250	0.00846	0.0024	118	70.9
Lilium Jet	0.0120	0.0030	83.7	47.5
Archer Maker	0.00451	0.0011	221	117
Bell Nexus 4EX	0.0113	0.0029	88.8	47.0
Pipistrel 801	0.00882	0.0021	113	61.2
Autoflight V1500	0.00810	0.0019	123	61.1

5 Summary

Ground infrastructure is an essential part of the emerging transportation system of UAM, which has received only secondary attention so far. In particular, the throughput capacities of vertiports are a research gap this article attempts to address. An existing MIP approach (see [32] for the method and [37] for preliminary studies) is applied to a range of vertiport scenarios to better understand throughput capacities and sensitivities. The approach considers four topologies to compute the optimal vertiport airfield layout for each scenario: single-pad, satellite, linear, and pier. Vertiport airfield areas from 100 to 10,000 m^2 are considered with *VoloCity* as the reference vehicle [53]. A baseline scenario is specified according to Preis et al. [51] with a turnaround time of 30 min at the gate. The summary of the vertiport sizing method and parameter values can be found in Sects. 2 and 3.1, respectively.

Next, the performance indicators "hourly passenger throughput per area" tp_{pax} and "area demand per hourly passenger throughput" tp_A are introduced (see Sect. 3.2). These allow for direct comparison of operational performance of different scenarios and vertiport sizes. The baseline case of the *VoloCity* results in $tp_{pax} = 0.0053$ PAX/h/m^2 and $tp_A = 188$ m^2/PAX/h. How these performance indicators, gate-to-pad ratios, and the choice of topologies varies is discussed in Sect. 3.3. In a second step, 13 prominent eVTOLs are investigated, and their maximum vehicle dimension and the number of seats is listed including a description of the deducted eVTOL design space (see Sect. 4.1). The consecutive studies presented in Sect. 4.2 showed that small vehicles (*CityAirbus*, *eHang 216*, and *Vahana*) perform best according to the above-defined indicators. The best performer is *CityAirbus* with a space requirement of 46.3 m^2/PAX/h and the worst performer is *Archer Maker* with a space requirement of 221 m^2/PAX/h. A comparison to other modes of transport is given in Appendix A.5.

The established insights can help three groups of people in the broader context of UAM. First, other researchers in academia can benefit from applying the rules-of-thumb for passenger throughput as input in their studies, in particular for making realistic vertiport capacity constraint assumptions in UAM demand studies. Second, vehicle developers can use the presented analysis to understand the operational performance of their own vehicle both individually and

in comparison with other vehicles. Beneficial operational environments are highlighted for different types of vehicles. Third, cities or communities can use the results as the first-order estimations and gain a feeling for the possible throughputs and space requirements a potential UAM service would have in their region.

6 Limitations and future work

The limitations of this article lie with the assumptions on one hand and with the interpretation of the results on the other hand. The following assumptions should find mention: first, all scenarios are based on a homogenous single-vehicle-type fleet. Vertiport design for mixed fleets would need to follow the largest vehicle type and thereby put smaller vehicles at a relative disadvantage. How this would impact vertiport airfield design and throughput capacity should be subject to further research. Second, the load factor of vehicles in Sect. 2 is assumed to be 1.0, which will most likely be lower in real-life operations. It can be expected that vehicles with less seats would benefit from this type of refined analysis as it is easier to pool fewer passengers and thereby more likely to fill up, e.g., two seats instead of five seats. Third, the feasibility of eVTOL designs was not accounted for except for the selection criterion of "prominent" designs (see Sect. 4.2). Once first eVTOLs have been certified, it is recommended to revisit the deducted design space and adjust it if needed.

Interpreting the results in a meaningful way is limited by two aspects: first, the FAA vertiport design guidelines are subject to ongoing change as discussed in Sect. 2 and new guidelines might impact the significance of presented results. Second, the assessment of operational performance in terms of hourly passenger throughput per area appears to take on a wide range of possible values. This variation can be explained by the discrete nature of vertiport layouts (see Sect. 3.3). It is therefore advised to express passenger throughput performance in the form of a value-range instead of a single value. These limitations could inform future research; two concrete publications are already planned as described in the following.

A planned publication will address the question of how passenger throughput capacity correlates with other performance indicators. Among these indicators will be the classical aircraft triad of speed, range, and payload, but also other ground operations-related indicators such as disk loading and rotor tip speed as indicators of noise. The goal will be to develop a holistic framework of performance assessment for eVTOLs with the throughput capacity as particular contribution from the authors.

Appendix

A.1 Parameter value specification for baseline scenario

In the following section, the aggregation of parameters as used in the baseline scenario (see Sect. 3.1 and Table 1) will be detailed. The parameter values are taken from Ref. [51] and the aggregation was first used in Ref. [52]. All indices of variables correspond to the IDs presented in Ref. [51].

Approach and landing time t_A (see Eq. 3) is the sum of process times for entering the airspace $t_{A,1} = 46.3$ s, final hover (and touch-down) $t_{A,2} = 22.9$ s, stopping the engines $t_{A,3} = 5.0$ s, and cool-down after landing $t_{A,4} = 30.0$ s. For the taxi-mode "hover", the engines are assumed to not be shut of wherefore t_A is shorter

$$t_A = t_{A,1} + t_{A,2}\left(+t_{A,3}\right) + t_{A,4} = 99.2s. \tag{3}$$

Take-off and departure time t_D (see Eq. 4) is the sum of process times for starting the engines $t_{D,1} = 4.5$ s, (take-off and) initial hover $t_{D,2} = 13.5$ s, leaving the airspace $t_{D,3} = 28.7$ s and cool-down after take-off $t_{D,4} = 30.0$ s. For the taxi-mode "hover", the engines are assumed to be already running wherefore t_D is shorter

$$t_D = \left(t_{D,1}+\right)t_{D,2} + t_{D,3} + t_{D,4} = 72.2s. \tag{4}$$

Boarding time $t_{B,in}$ (see Eq. 5) is the sum of process times for the passenger entering the gate (included walking into the proximity of the vehicle) $t_{B,2} = 19.7$ s and boarding the vehicle $t_{B,3} = 13.5$ s. De-boarding time $t_{B,out}$ (see Eq. 6) is the sum of process times for the passenger de-boarding the vehicle $t_{B,4} = 65.8$ s and leaving the gate (included leaving the proximity of the vehicle) $t_{B,5} = 26.7$ s

$$t_{B,in} = t_{B,2} + t_{B,3} = 92.7s \tag{5}$$

$$t_{B,out} = t_{B,4} + t_{B,5} = 92.5s. \tag{6}$$

A.2 Forming throughput performance indicators

Section 3.2 defines the throughput performance indicators tp_{pax} and tp_A. In Fig. 5, the process of how the indicators are formed and then aggregated into rules-of-thumb is visualized for the reference vehicle *VoloCity*. For further reference, the same process will also be illustrated for *eHang 216* (Fig. 11) and *Joby S4* (Fig. 12) in the following.

A.3 How-to apply throughput performance indicators

This article introduced two throughput performance indicators to measure operational efficiency on the ground: "hourly passenger throughput per area" tp_{pax} and the reciprocal of "area demand per hourly passenger throughput" tp_A. In this appendix examples will be given to help apply the indicators as rules-of-thumb for vertiport sizing.tp_{pax} can be used to estimate the possible hourly passenger throughput on a given area (from area to throughput). Say the available area A has 3000 m^2 (e.g., 100 by 30 m), there is no charging intended and a *VoloCity* should be operated on it. In this case, Table 2 can serve as look-up table: with a median throughput capacity of $tp_{pax,median} = 0.0123$ PAX/h/m^2, the throughput is estimated to be $TP_{pax} = tp_{pax}$ x $A = 36.9$ *PAX/h*. Rounded down to the next natural 36 passengers will be catered per hour in the presented scenario. In a second step to reduce the risk of error, a range of throughput capacities could be given, for example from $tp_{pax,5\%} = 0.0079$ PAX/h/m^2 to $tp_{pax,95\%} = 0.0189$ PAX/h/m^2. Doing the same calculation for each, it can be said that with a 90% confidence (between 5 and 95%), the range of passengers that can be catered per hour is 23–56.tp_A can be used to determine the space requirement for a desired throughput capacity (from throughput to area). Say the desired hourly passenger throughput $TP_{pax} = 50$ PAX/h and a charging time of 30 min is assumed. In this case, Table 5 can serve as look-up table: with a space demand of $tp_{A,Joby} = 82.4$ m^2/PAX/h, the *Joby S4* vehicle would require a total area of $A_{Joby} = tp_{A,Joby}$ x $TP_{pax} = 4120$ m^2. In a second step, the required area could be compared to other vehicles; for example, *Beta ALIA-250* and *eHang 216*. With space demands of $tp_{A,Beta} = 118$ m^2/PAX/h and $tp_{A,eHang} = 49.7$ m^2/PAX/h, this would lead to a total area of 5900 m^2 for *Beta*'s vehicle and 2485 m^2 for *eHang*'s vehicle.

A.4 Dimensions of vertiport airfield elements

Dimensions of pads, gates, and taxi-ways are driving the layout and design of vertiport airfields (see Sect. 4.1). For the purpose of this article, the relevant dimensions are derived from the FAA "Heliport Design Guidelines" [49] (see Fig. 13) and their relationship to the maximum dimensions of the vehicle is visualized below (Fig. 14). In contrast to the main body of the article, the heliport guidelines are also used to visualize the pad dimensions, so that the comparison rests on an established body of guidelines (as explained in

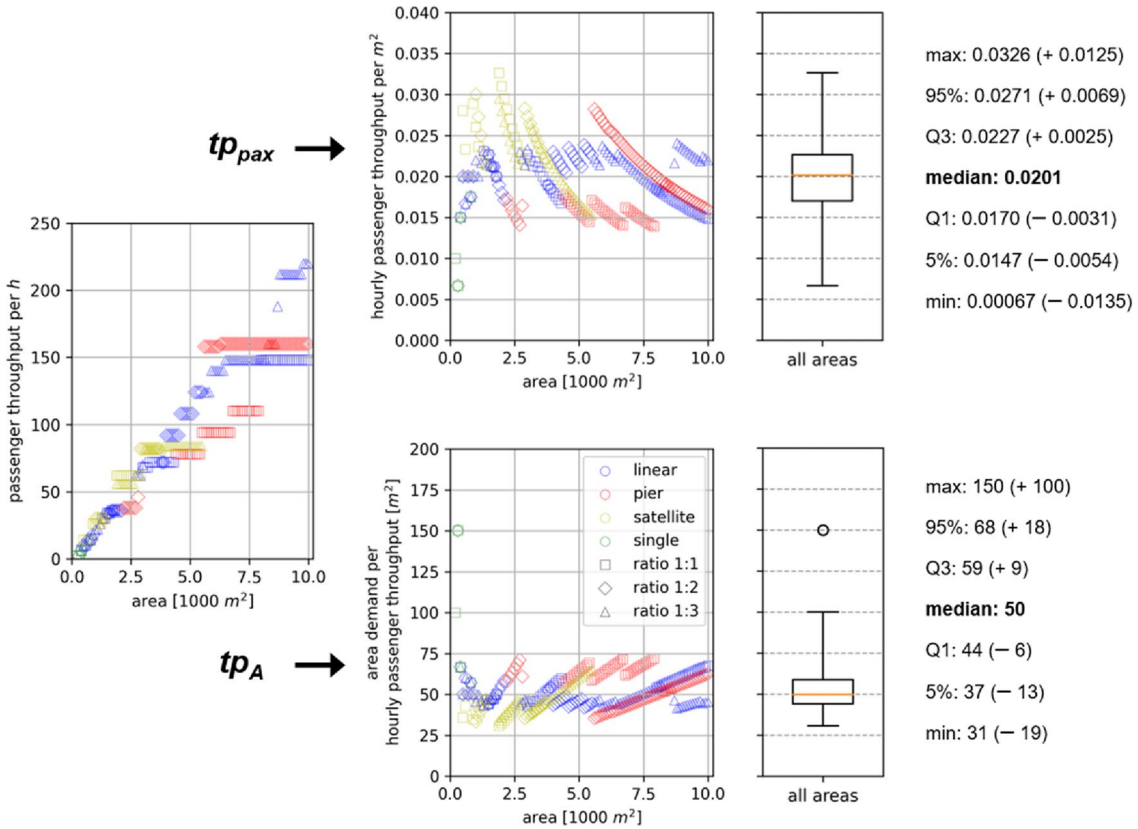

Fig. 11 Throughput performance indicators and rules-of-thumb for eHang 216

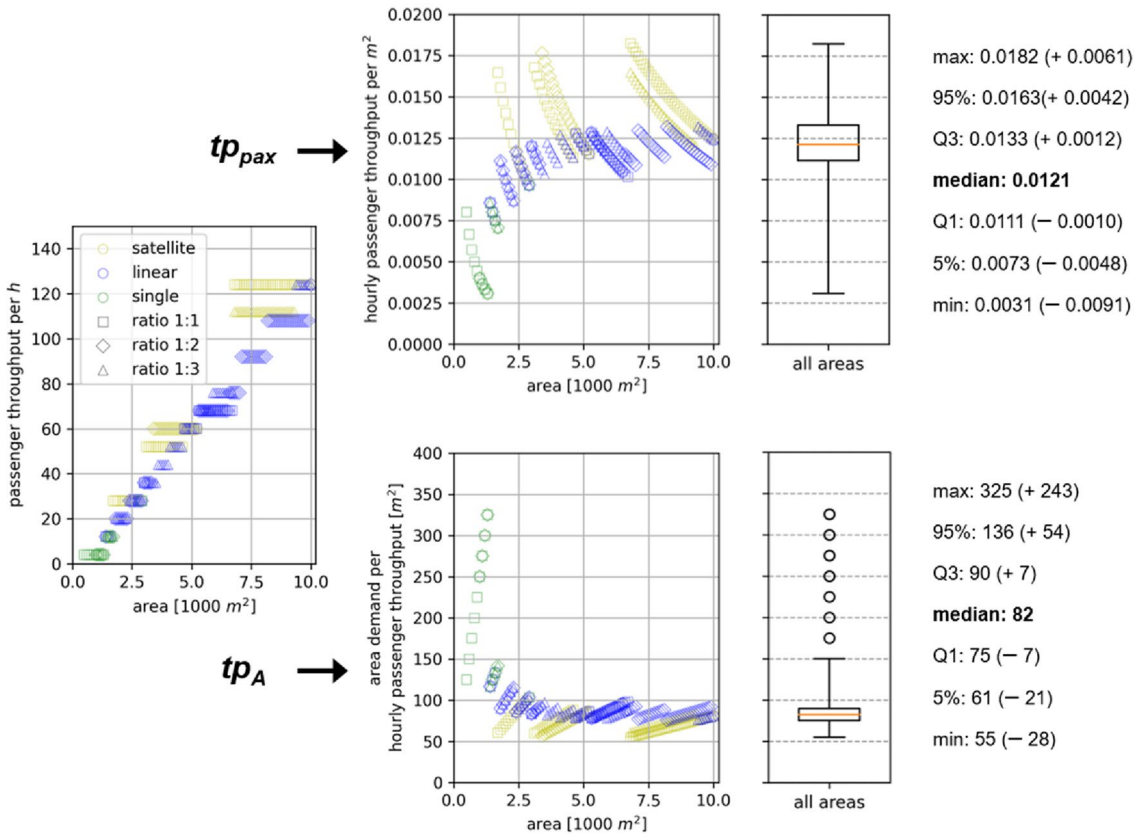

Fig. 12 Throughput performance indicators and rules-of-thumb for Joby S4

Sect. 2, the studies in this article use the pad dimensions given by the newly released FAA vertiport guidelines [48]).

For pads, the side length and area of the three squares (TLOF, FATO, and Pad Safety) is displayed below. For gates, the diameter and area of the two circles (Gate Area and Gate Safety) is displayed with differentiated measures depending on the taxi-mode (hover or ground). For taxi-ways, the width and area of a segment between two gates is displayed, also distinguishing between taxi-modes.

Finding the best gate-to-pad ratio is an important factor in choosing the optimal vertiport layout, as was hinted on in Sect. 2.4. The quotient of pad safety to gate safety is shown in Fig. 15. Different safety standards apply for gates (and taxi-ways) depending on the taxi-mode, which are treated in detail in the previous publication by Preis [32]. As can be seen, there is a trade-off between the modes of taxi at around 9 m of maximum vehicle dimension. Generally speaking, the slopes of both curves are falling, which can be interpreted as gates being more performant according to tp_{pax} for small vehicles compared to large vehicles, when being in the trade-off situation with pads. Or, in other words, small vehicle operators have an interest in freeing up pads quickly, because they are more "space-costly" in relative terms. The quotient shown in

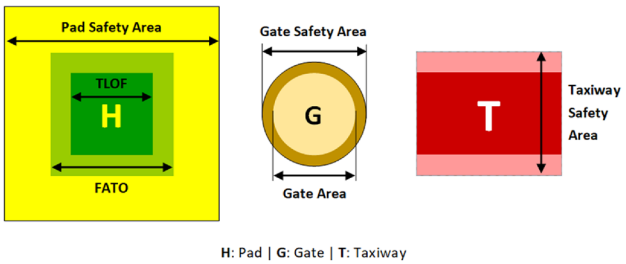

Fig. 13 Dimensions of pads, gates, and taxi-ways

Fig. 15 is the number of gates that would fit into the same area as one pad.

A.5 Comparing space demands of transport modes

Throughout this article, the space demands for different transport modes are mentioned, which will be directly compared in this section. There are three sources that will be compared: first, the space demand of existing modes of transport (see Sect. 1); second, area requirements for vertiports as estimated in the scientific literature (see Sect. 2);

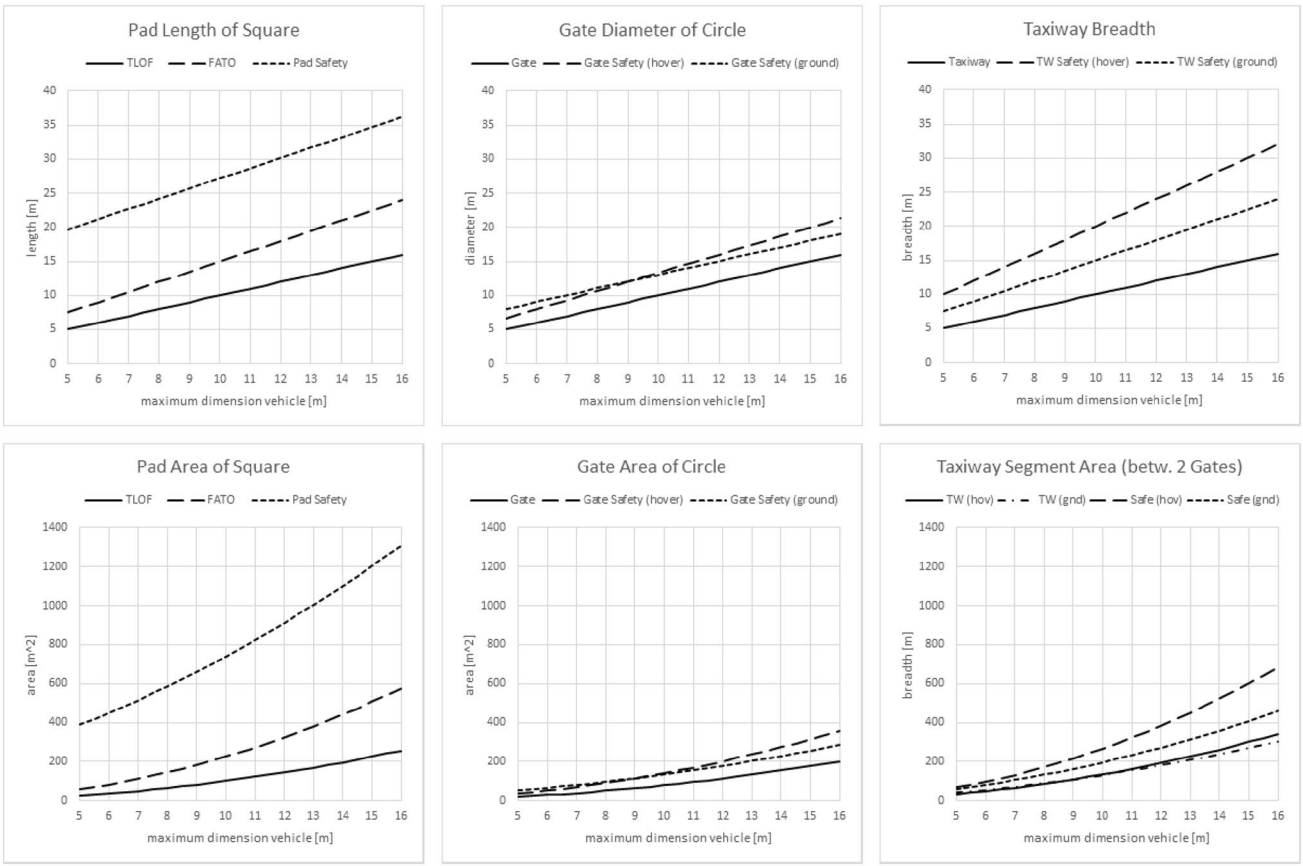

Fig. 14 Visualization of length and area of vertiport elements

and third, the area demand of various eVTOL designs as calculated in this article (see Sect. 4.2). A comparative summary of all space demands is shown in Table 6. Before listing the transport modes, the following key assumption needs to be emphasized: the space demand for eVTOLs is purely based on the airfield and does not consider the passenger terminal or other UAM facilities.

To easily compare the transport modes, the space demands will all transformed into the unit *square-meters per hourly passenger*. First, the numbers for existing modes of transport are given as space demand per *daily* passenger. Assuming a bi-model distribution with a morning and afternoon peak, Ref. [66] showed that between 12 and 15% (median 13.5%) of the total daily traffic occurs during a typical peak hour. This means that the number of daily passengers is 7.4 times the number of (maximum) hourly passengers. Applying this factor to transform daily into hourly space demand leads to a 7.4 times higher space demand when wanting to cater the same number of passengers in an hour compared to a full day. Concretely, this results in a space demand per *hourly* passenger of 481 m^2 for cars (65

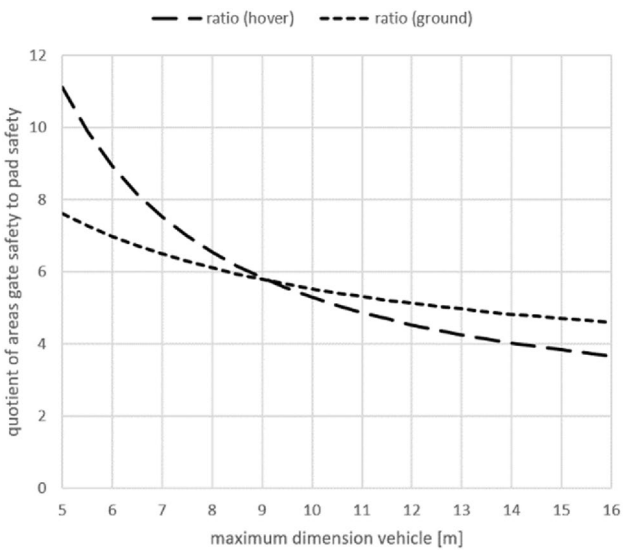

Fig. 15 Comparing areas of pad safety and gate safety

Table 6 Comparison of space demands for existing modes of transport and estimated area demands of eVTOLs

Transport mode	Space demand [m^2/PAX/h]	Source
Rail	237	Existing infrastructure
Car	481	Existing infrastructure
Aviation	4588	Existing infrastructure
eVTOLs	105	Estimation in literature
City Airbus	46	Own estimation
Archer Maker	221	Own estimation

m^2 per daily passenger), 237 m^2 for rail (32 m^2 per daily passenger), and 4588 m^2 for airplanes (620 m^2 per daily passenger). Next, the area requirement for eVTOLs in the scientific literature will be considered where Ref. [41] states 420 m^2 per hourly *vehicle* throughput. The number of seats is not specified wherefore four seats will be assumed corresponding to the median number of seats in the review of prominent eVTOL designs in Table 4. Applying Eqs. 1 and 2 leads to a space requirement per hourly *passenger* of 105 m^2. Finally, to indicate the range of results from the different eVTOL designs that were studied in this article, the highest and lowest area demands were selected from the results presented in Table 5: *City Airbus* with 46 m^2/PAX/h and *Archer Maker* with 221 m^2/PAX/h. The comparison in Table 6 shows that eVTOLs have the smallest space demand of all transport modes—this insight needs to be interpreted, as mentioned above, in light of the assumption that only the vertiport *airfield* was considered.

Funding Open Access funding enabled and organized by Projekt DEAL.

Declarations

Conflict of interest The authors declare that they have no conflict of interest.

Data availability All eVTOL-related data is available under the respective URLs.

Code availability MATLAB code can be made available upon personal request to lukas.preis@tum.de.

References

1. Vascik, P.D.: Systems analysis of urban air mobility operational scaling. Ph.D., Department of Aeronautics & Astrophysics, Massachusetts Institute of Technology (MIT), Cambridge. https://dspace.mit.edu/handle/1721.1/128057 (2020). Accessed 17 Dec 2022
2. National Aeronautics and Space Administration (NASA), Ed.: UAM Vision Concept of Operations (ConOps) UAM Maturity Level (UML) 4: Version 1.0. https://ntrs.nasa.gov/citations/20205011091 (2020) Accessed 13 Jul 2022
3. Schuchardt, B.I., et al.: Urban air mobility research at the DLR German Aerospace Center—getting the HorizonUAM project started. In: AIAA Aviation 2021 Forum, virtual event, p. 361. https://arc.aiaa.org/doi/abs/10.2514/6.2021-3197 (2021) Accessed 13 Jul 2022
4. Vascik, P.D. Hansman, J.R.: Scaling constraints for urban air mobility operations: air traffic control, ground infrastructure, and noise. In: 18th AIAA Aviation Technology, Integration, and Operations Conference 2018, Atlanta. https://arc.aiaa.org/doi/10.2514/6.2018-3849 (2018) Accessed 18 Dec 2022
5. Vascik, P.D., Hansman, J.R.: Constraint identification in on-demand mobility for aviation through an exploratory case study of Los Angeles. In: 17th AIAA Aviation Technology, Integration, and Operations Conference, Denver. https://arc.aiaa.org/doi/10.2514/6.2017-3083 (2017) Accessed 18 Dec 2022
6. Shamiyeh, M., Bijewitz, J., Hornung, M.: A review of recent personal air vehicle concepts. In: 6th CEAS Conference. https://www.icas.org/ICAS_ARCHIVE/ICAS2018/data/papers/ICAS2018_0794_paper.pdf (2017) Accessed 18 Dec 2022
7. Liu, Y., Kreimeier, M., Stumpf, E., Zhou, Y., Liu, H.: Overview of recent endeavors on personal aerial vehicles: a focus on the US and Europe led research activities. Prog. Aerosp. Sci. **91**, 53–66 (2017). https://doi.org/10.1016/j.paerosci.2017.03.001
8. Lineberger, R., Hussain, A., Mehra, S., Pankratz, D.M.: Elevating the future of mobility: Passenger drones and flying cars. Deloitte Insights. https://www2.deloitte.com/us/en/insights/focus/future-of-mobility/passenger-drones-flying-cars.html (2018). Accessed 2 May 2023
9. Zhou, Y., Zhao, H., Liu, Y.: An evaluative review of the VTOL technologies for unmanned and manned aerial vehicles. Comput. Commun. **149**(2), 356–369 (2020). https://doi.org/10.1016/j.comcom.2019.10.016
10. Giligan, M., Grizzle, J.D., Cox, V.H.: Integration of unmanned aircraft systems into the national airspace system: concept of operations v2.0. Federal Aviation Administration (2012)
11. Kopardekar, P.H.: Unmanned aerial system (UAS) traffic management (UTM): enabling low-altitude airspace and UAS operations. NASA Ames Research Center, Moffett Field, California NASA/TM—2014–218299. https://ntrs.nasa.gov/api/citations/20140013436/downloads/20140013436.pdf (2014) Accessed 13 Jun 2022
12. European Union Aviation Safety Agency (EASA), Ed.: Concept of Operations for Drones: a risk based approach to regulation of unmanned aircraft. https://www.easa.europa.eu/en/document-library/general-publications/concept-operations-drones (2015). Accessed 2 May 2023
13. Balakrishnan, K., Polastre, J., Mooberry, J., Golding, R., Sachs, P.: Blueprint For The Sky: The roadmap for the safe integration

of autonomous aircraft. https://www.airbusutm.com/uam-resources-airbus-blueprint (2018) Accessed 13 Jun 2022
14. Geister, G., Korn, B.: Concept for urban airspace integration DLR U-space blueprint: integrating UAS into the future aviation system. Deutsches Zentrum für Luft- und Raumfahrt (DLR). https://www.dlr.de/de/medien/publikationen/sonstige-publikationen/2017/blueprint-concept-for-urban-airspace-integration_2933 (2017). Accessed 2 May 2023
15. Federal Aviation Administration (FAA), Ed.: Low altitude authorization and notification capability (LAANC) concept of operations. https://www.faa.gov/uas/programs_partnerships/data_exchange/laanc_for_industry/media/laanc_concept_of_operations.pdf (2017) Accessed 13 Jun 2022
16. Federal Aviation Administration (FAA) and U.S. Department of Transportation (DoT), Eds.: Urban air mobility (UAM): concept of operations v1.0. https://nari.arc.nasa.gov/sites/default/files/attachments/UAM_ConOps_v1.0.pdf (2020) Accessed 15 Nov 2022
17. Thipphavong, D.P. et al.: Urban air mobility airspace integration concepts and considerations. In: 18th AIAA aviation technology, integration, and operations conference 2018, Atlanta, p. 2018. https://arc.aiaa.org/doi/10.2514/6.2018-3676 (2018) Accessed 16 Nov 2022
18. European Union Aviaton Safety Agency (EASA), Ed.: U-space regulatory framework workshop: summary of conclusions. https://www.easa.europa.eu/en/newsroom-and-events/events/u-space-workshop-2019 (2019). Accessed 2 May 2023
19. Sparrow, V., et al.: Aviation noise impacts white paper: state of the science 2019: aviation noise impacts. https://www.icao.int/environmental-protection/Documents/Noise/ (2019)
20. Vascik, P.D., Hansman, J.R.: Evaluation of key operational constraints affecting on-demand mobility for aviation in the Los Angeles basin: ground infrastructure, air traffic control and noise. In: 17th AIAA Aviation Technology, Integration, and Operations Conference, Denver. https://arc.aiaa.org/doi/10.2514/6.2017-3084 (2017) Accessed 18 Dec 2022
21. International Transport Forum (ITF) and Organisation for Economic Co-operation and Development (OECD), Eds.: Ready for take-off?: Integrating drones into the transport system. https://www.itf-oecd.org/integrating-drones-transport-system (2021) Accessed 13 Jun 2022
22. Ackerman, K.A., Gregory, I.M.: Trajectory generation for noise-constrained autonomous flight operations. In: AIAA Scitech 2020 Forum, Orlando. https://arc.aiaa.org/doi/10.2514/6.2020-0978 (2020) Accessed 2 May 2023
23. Phiesel, D., Moormann, D.: Bewertung des Bodenrisikos beim Betrieb von kleinen unbemannten Fluggeräten: Ein einfacher und quantitativer Ansatz. In: 66. Deutscher Luft- und Raumfahrtkongress: DLRK 2017, München. http://publications.rwth-aachen.de/record/713024 (2017) Accessed 2 May 2023
24. Duwe, D., Sprenger, A.: Acceptance, preferences and willingness to pay analysis for flying cars and passenger drones. In: 6th International Conference on Innovation in Science and Technology, London. https://www.dpublication.com/abstract-of-6th-ist/6-f220/ (2019) Accessed 18 Dec 2022
25. Bonk R., et al.: Fit2Fly: a proof of concept for testing the commercial feasibility of unmanned aerial system operations. In: AIAA Scitech 2020 Forum, Orlando. https://arc.aiaa.org/doi/10.2514/6.2020-0740 (2020) Accessed 2 May 2023
26. Straubinger, A., Rothfeld, R.L., Shamiyeh, M., Büchter, K.-D., Kaiser, J., Plötner, K.O.: An overview of current research and developments in urban air mobility—setting the scene for UAM introduction. JATM **87**, 101852 (2020). https://doi.org/10.1016/j.jairtraman.2020.101852
27. Garrow, L.A., German, B.J., Leonard, C.E.: Urban air mobility: a comprehensive review and comparative analysis with autonomous and electric ground transportation for informing future research. Transportation Research Part C: Emerging Technologies **132**(2), 103377 (2021). https://doi.org/10.1016/j.trc.2021.103377
28. Cohen, A., Guan, J., Beamer, M., Dittoe, R., Mokhtarimousavi, S.: Reimagining the future of transportation with personal flight: preparing and planning for urban air mobility. https://escholarship.org/uc/item/9hs209r2 (2020) Accessed 2 May 2023
29. Volocopter, Ed.: The Roadmap to scalable Urban Air Mobility: White Paper 2.0. Bruchsal. http://www.volocopter.com/content/uploads/20210324_Volocopter_WhitePaper_Roadmap_to_scalable_UAM_m.pdf (2021) Accessed 3 May 2021
30. Rajendran, S., Srinivas, S.: Air taxi service for urban mobility: a critical review of recent developments, future challenges, and opportunities. Transportation Research Part E: Logistics and Transportation Review **143**(2), 102090 (2020). https://doi.org/10.1016/j.tre.2020.102090
31. Schweiger, K., Preis, L.: Urban air mobility: systematic review of scientific publications and regulations for vertiport design and operations. Drones **6**(7), 179 (2022). https://doi.org/10.3390/drones6070179
32. Preis, L.: Quick sizing, throughput estimating and layout planning for VTOL aerodromes—a methodology for vertiport design. In: AIAA aviation 2021 forum, virtual event. https://arc.aiaa.org/doi/10.2514/6.2021-2372 (2021)
33. Allianz pro Schiene: Schiene spart Fläche und lässt Natur ihren Raum: Straße beansprucht über zwölfmal so viel Platz pro beförderter Person, Berlin. https://www.allianz-pro-schiene.de/presse/pressemitteilungen/schiene-spart-flaeche-und-laesst-natur-ihren-raum/ (2021) Accessed 28 Sep 2022
34. Umwelt Bundesamt: Struktur der Flächennutzung. Dessau-Roßlau. https://www.umweltbundesamt.de/daten/flaeche-boden-land-oekosysteme/flaeche/struktur-der-flaechennutzung (2021) Accessed 28 Sep 2022
35. Statistisches Bundesamt: Flächennutzung: Bodenfläche insgesamt nach Nutzungsarten in Deutschland. https://www.destatis.de/DE/Themen/Branchen-Unternehmen/Landwirtschaft-Forstwirtschaft-Fischerei/Flaechennutzung/Tabellen/bodenflaeche-insgesamt.html;jsessionid=D665CB09025A44A215F0DE6E63EB97FB.live731. Accessed 28 Sep 2022
36. Statistisches Bundesamt: Personenverkehr: Beförderte Personen in Deutschland. https://www.destatis.de/DE/Themen/Branchen-Unternehmen/Transport-Verkehr/Personenverkehr/Tabellen/befoerderte-personen.html;jsessionid=494BFE665DF01352011B0A0AE3FD716F.live731. Accessed 28 Sep 2022
37. Preis, L., Hack Vazquez, M.: Vertiport throughput capacity under constraints caused by vehicle design, regulations and operations. In: Delft International Conference on Urban Air-Mobility (DIC-UAM), Delft/virtual. http://cdn.aanmelderusercontent.nl/i/doc/8fa60b7fcfa71ea900ce2bea2037a151?forcedownload=True (2022) Accessed 5 Apr 2022
38. Vascik, P.D., Hansman, J.R.: Development of vertiport capacity envelopes and analysis of their sensitivity to topological and operational factors. In: AIAA Scitech 2019 Forum, San Diego. http://arc.aiaa.org/doi/10.2514/6.2019-0526 (2019) Accessed 18 Dec 2022
39. Zelinski, S.: Operational analysis of vertiport surface topology. In: 39th DASC—Digital Avionics Systems Conference: Virtual conference, October 11–16, 2020: 2020 conference proceedings, San Antonio. http://ieeexplore.ieee.org/document/9256794 (2020) Accessed 18 Dec 2022
40. Feldhoff, E., Soares Roque, G.: Determining infrastructure requirements for an air taxi service at Cologne Bonn Airport. CEAS, pp. 1–13, (2021) https://doi.org/10.1007/s13272-021-00544-4
41. Taylor, M., Saldanli, A., Park, A.: Design of a vertiport design tool. In: 2020 Integrated Communications Navigation and Surveillance Conference (ICNS), Herndon. http://ieeexplore.ieee.org/document/9222989 (2020) Accessed 18 Dec 2022

42. Petersen, J.D., Alexander, R.J., Swaintek, S.S.: Dynamic Vertiport Configuration. US 2020/0226937 A1, USA 16 / 248,170, Jun 16. https://patentimages.storage.googleapis.com/4b/a8/76/10e71cb3d92091/US20200226937A1.pdf (2020) Accessed 18 Dec 2022
43. International Organization for Standardization (ISO): ISO/AWI 5491: Vertiports—Infrastructure and equipment for Vertical Take-Off and Landing (VTOL) of electrically powered cargo Unmanned Aircraft System (UAS). http://www.iso.org/standard/81313.html. Accessed 1 Jun 2021
44. Lineberger, R., Hussain, A., Metcalfe, M., Rutgers, V.: Infrastructure barriers to the elevated future of mobility: Are cities ready with the infrastructure needed for urban air transportation? Deloitte Insights. https://www2.deloitte.com/us/en/insights/focus/future-of-mobility/infrastructure-barriers-to-urban-air-mobility-with-VTOL.html (2019)
45. Lilium: Designing a scalable vertiport: taking the sci-fi vision of landing pads and turning it into a realistic and affordable transit option. https://blog.lilium.com/designing-a-scalable-vertiport-c12e75be1ec5
46. Johnston, T., Riedel, R., Sahdev, S.: To take off, flying vehicles first need places to land: the buzz about vehicles flying above hides the infrastructure challenge below. https://www.mckinsey.com/industries/automotive-and-assembly/our-insights/to-take-off-flying-vehicles-first-need-places-to-land (2020) Accessed 18 Dec 2022
47. Hack Vazquez, M.: Vertiport Sizing and Layout Planning through Integer Programming in the Context of Urban Air Mobility. Master thesis, Technical University of Munich (TUM), Munich. https://mediatum.ub.tum.de/node?id=1624149 (2021) Accessed 2 May 2023
48. Federal Aviation Administration (FAA), Ed.: Engineering Brief No. 105, Vertiport Design. https://www.faa.gov/newsroom/faa-releases-vertiport-design-standards-support-safe-integration-advanced-air-mobility (2022) Accessed 28 Sep 2022
49. Federal Aviation Administration (FAA): Heliport Design. AC 150/5390–2C. https://www.faa.gov/airports/resources/advisory_circulars/index.cfm/go/document.current/documentnumber/150_5390-2 (2012) Accessed 13 Jun 2022
50. European Union Aviaton Safety Agency (EASA): Second Publication of Proposed Means of Compliance with the Special Condition VTOL. MOC-2 SC-VTOL. https://www.easa.europa.eu/en/downloads/136697/en (2022) Accessed 28 Sep 2022
51. Preis, L., Hornung, M.: Vertiport operations modeling, agent-based simulation and parameter value specification. Electronics **11**(7), 1071 (2022). https://doi.org/10.3390/electronics11071071
52. Preis, L., Cheng, S.: Simulation of individual aircraft and passenger behavior and study of impact on vertiport operations. In: AIAA Aviation 2022 Forum, Chicago. https://arc.aiaa.org/doi/abs/10.2514/6.2022-4074 (2022)
53. Volocopter: VoloCity: Design specifications. Calculated approximations not yet tested in flight. https://www.volocopter.com/solutions/volocity/ (2019) Accessed 22 Jul 2021
54. AIRBUS: Airbus CityAirbus. https://transportup.com/airbus-cityairbus/. Accessed 22 Dec 2021
55. Joby Aviation: Joby S4. https://www.jobyaviation.com/ Accessed 21 Dec 2021
56. AIRBUS: Vahana: Our single-seat eVTOL demonstrator. https://www.airbus.com/en/innovation/zero-emission/urban-air-mobility/vahana. Accessed 21 Dec 2021
57. Wisk: Discover the Future of Urban Air Mobility. https://wisk.aero/aircraft/. Accessed 14 Sep 2022
58. eHang: EHang AAV: The Era of Urban Air Mobility is Coming. https://www.ehang.com/ehangaav. Accessed: 21 Dec 2021
59. UBER Elevate: UberAir Vehicle Requirements and Missions. https://s3.amazonaws.com/uber-static/elevate/Summary+Mission+and+Requirements.pdf (2018) Accessed 5 Oct 2021
60. BETA Technologies: Aircraft ALIA-250. https://www.beta.team/aircraft/ Accessed 11 Feb 2022
61. Nathen, P., Bardenhagen, A., Strohmayer, A., Miller, R., Grimshaw, S., Taylor, J.: Architectural performance assessment of an electric vertical take-o and landing (e-VTOL) aircraft based on a ducted vectored thrust concept. https://lilium.com/files/redaktion/refresh_feb2021/investors/Lilium_7-Seater_Paper.pdf (2021) Accessed 21 Dec 2021
62. Archer: Maker 101: Introducing Maker. https://www.archer.com/maker. Accessed 14 Sep 2022
63. Bell: Bell Nexus. https://de.bellflight.com/products/bell-nexus. Accessed 14 Sep 2022
64. Pipistrel: 801 EVTOL. https://www.futureflight.aero/aircraft-program/801-evtol. Accessed 14 Sep 2022
65. Autoflight: Prosperity I: Next Generation Manned eVTOL. https://www.autoflight.com/en/products/. Accessed 14 Sep 2022
66. Preis, L., Hornung, M.: A vertiport design heuristic to ensure efficient ground operations for urban air mobility. Appl. Sci. **12**(14), 7260 (2022). https://doi.org/10.3390/app12147260